A Wheeling-Hopping Combination Scout Robot

Jie Zhao, Gangfeng Liu, Qinghu Han, and Hegao Cai

State Key Laboratory of Robotic Technology and System,Harbin Institute of Technology, Harbin, 150001, P. R. China
liugangfeng@hit.edu.cn

Abstract. A hopping robot can jump over the barrier several times higher than its own height. The combination of the hopping movement and the wheeling movement can greatly enhance the scope of robot's activities. In this paper, a novel five-shank hopping mechanism was employed to build the wheeling-hopping combination scout robot. The nonlinear character of the five-shank hopping mechanism was analyzed and then used in the proposed nonlinear spring-mass model for the robot. The rules of robot's movement were deduced, influencing factors of the jumping height were analyzed and the countermeasure was adopted. Finally, a simulation analysis and an experiment of the robot's movement were carried out. The results showed that the robot has strong locomotivity and survival ability.

Keywords: Scout Robot, the Five-shank Hopping Mechanism, Nonlinear Spring-mass Model.

1 Introduction

At present the types of moving robot include wheeling, walking, tracking and so on. Wheeling movement is constrained by the roughness of relief, while walking movement is flexible and it is complicated to control all the walking attitudes. Even the tracking movement becomes useless when a barrier bigger than its own size is encountered. Used in searching after disaster, interstellar probe, military scouting and anti-terrorism activities, robots need strong locomotivity and survival ability to satisfy the more complicated environment, miscellaneous barriers and dangers. The hopping robot can jump over the barrier several and even ten times higher than its own height, and hopping movement with the sudden outbreak can help to avoid danger. Many foreign institutes begin to research on the hopping robot because of its unique merit. For example, NASA together with California Institute of Technology developed a frog-like hopping robot, and Sandia National Lab of USA designed a hopping robot for minesweeping in the army. Besides, University of Minnesota and Massachusetts Institute of Technology respectively built hopping robots for further research.

In this paper, wheeling movement and hopping movement were combined to build a wheeling-hopping combination scout robot. A novel five-shank hopping mechanism was employed in the robot, and its nonlinear character was used in the proposed nonlinear spring-mass model for the robot. The rules of robot's movement were deduced, and a simulation analysis and an experiment of the robot's movement were carried out.

C. Xiong et al. (Eds.): ICIRA 2008, Part I, LNAI 5314, pp. 973–981, 2008.

2 Brief Account of the Wheeling-Hopping Combination Robot and Design of the Hopping Mechanism

Mechanical system of the wheeling-hopping combination scout robot is composed of two-wheel driving assembly and a hopping assembly. The robot can be driven through flat terrain to the destination by the wheeling assembly. When facing barrier or ditch, the robot manipulated by the hopping mechanism can jump over the obstacle.

The wheel driving assembly of the robot has two independent drive wheels. And the structure of the hopping assembly is shown in Fig 1.

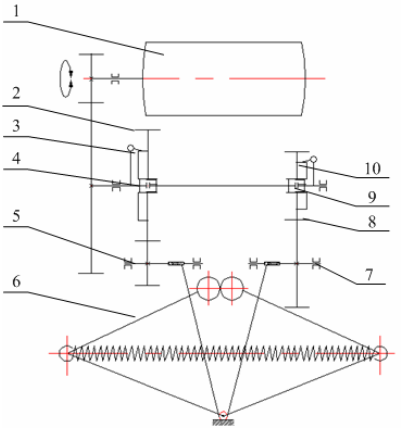

1-Gear motor ; 2-Partial gear drive ; 3-Ratchet-and-pawl ; 4-One-way bearing ; 5-Releasing reel ; 6-Five-shank hopping mechanism ; 7-Regulating reel ; 8-All-gear drive ; 9-One-way bearing ; 10-Ratchet-and-pawl

Fig. 1. Structure of the hopping mechanism

The hopping mechanism is composed of gear motor 1, energy-releasing mechanism (including 2, 3, 4, 5), five-shank hopping mechanism 6 and energy-regulating mechanism (including 7, 8, 9, 10). When the gear motor is in positive revolutions, one-way bearing 9 and gear 8 are driven to regulate the reel 7, and then the extension of the spring, thus the energy storage is changed. When the gear motor is in negative revolutions, one-way bearing 4 and partial gear 2 are driven to regulate the reel 5, and then fine-tune the extension of the spring, or release the string. Then the five-shank hopping mechanism exerts the force on the ground and the robot jumps up. Ratchet-and-pawl 3 and 10 lock the energy-releasing mechanism and energy-regulating mechanism separately at any position. The energy-regulating mechanism can rotate continuously to regulate the energy storage in a wide range. And the energy- releasing mechanism can easily release the spring to get the robot jumping. The robot has a small figure of $\phi 110 \times 150\,\text{mm}$, and it weights 1.12kg.

3 Analysis of the Five-Shank Hopping Mechanism

The hopping mechanism is the key part of the scout robot. The performance of six-shank mechanism is analyzed in [3], and it was pointed out that the six-shank mechanism helped to lower the requirement for the single spring and avoid the spring's buckling. Also, the non-linear relationship between spring's force and deformation can be favorable to prevent robot from jumping ahead of time. In this paper, a five-shank mechanism is used to build the hopping robot, as Fig 2 showed.

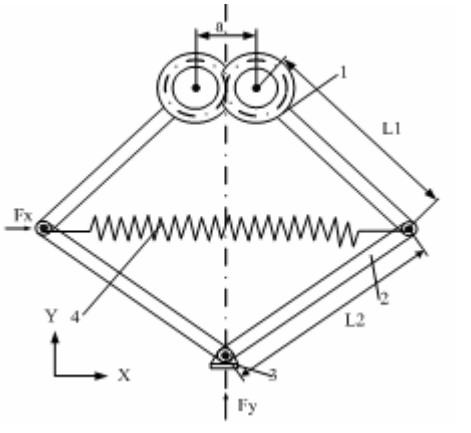

Fig. 2. Schematic diagram of the five-shank mechanism

The mechanism expands in direction Y. According to the principle of virtual work, the relation between acting force and deformation is $F_y \cdot dy = F_x \cdot dx$. Associating geometrical relationship of the five-shank mechanism, equations set can be derived as follows:

$$\begin{cases} F_y = \dfrac{-k(x - L_0)\cdot(y\cdot c - c^2)}{\dfrac{x}{2}\cdot c - (y-c)(\dfrac{a}{2} - \dfrac{x}{2})}, \\ L_2^2 = (\dfrac{x}{2})^2 + (y-c)^2, \\ c = \sqrt{L_1^2 - (\dfrac{x}{2} - \dfrac{a}{2})^2}. \end{cases} \tag{1}$$

Where k is the elastic coefficient of spring, L_0 is the original length of spring, and c is intermediate variable. When the real parameter of the robot was substituted, the relation between acting force and deformation of the five-shank mechanism in direction Y is shown in Fig 3.

It was found that the relation between acting force and deformation of the five-shank mechanism is similar to that of the six-shank mechanism derived in [3]. But the former has more simple structure, and can be easily operated with only one DOF.

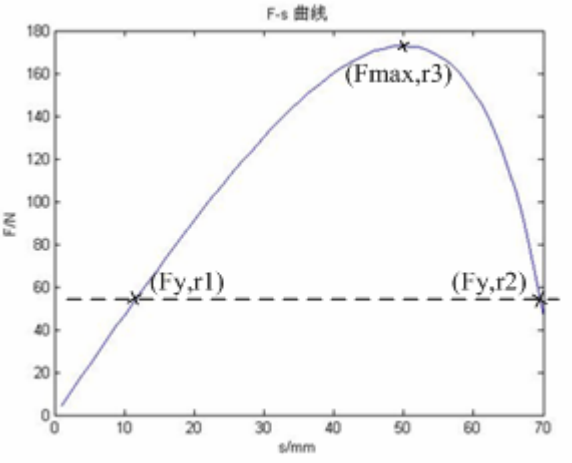

Fig. 3. F_y-Y curve of the five-shank mechanism

Thus in this paper, the five-shank mechanism is adopted, and the relation between its acting force and deformation is simplified by curve fitting method as：

$$F_y^* = Ky(1 - \frac{b}{\sqrt{4a^2 - y^2}}). \tag{2}$$

In it, K, a and b are the parameters of the fitting curve. $K = 5, b = 25, a = 42.5$ were got when it was set as $k = 5, L_0 = 30, L_1 = 40, L_2 = 45$.

Assume that the length of the five-shank mechanism in direction Y is y_0 When the spring has no deformation. According to Hooke's law, the equivalent elastic coefficient of the non-linear spring produced by the five-shank mechanism is:

$$K(y) = F_y^* / (y - y_0). \tag{3}$$

4 Analysis on the Dynamic Model of the Robot

In order to get the jumping performance of the five-shank mechanism, it is necessary to establish the dynamic model of the robot. At present the jumping model can be divided into two kinds: spring-single mass continuous jumping model and spring-double mass intermittent jumping model. The former refills the energy of jumping and adjusts the robot's attitudes dynamically, and then goes on with the next jump after landing. So the continuous equation of motion can be set up for this model. But using this model, it is difficult for the robot to balance in quiescent condition. Also, the horizontal distance is limited because of the front rake which is hard to control, as a result the robot is always assumed to be vertical before jumping. The latter has two mass connected by a spring. The bottom mass balances and stabilizes the whole robot. After landing the robot refills energy of jumping and adjusts its attitudes according to the circumstance, and gets ready for the next jump. This model is more practical for the robot mentioned above.

The wheeling-hopping combination scout robot built in this paper stores energy from the extension of spring driven by the motor, which obviously belongs to intermittent jumping model. Meanwhile, the upper part of the robot is much heavier than the supporting leg of the five-shank mechanism, so single mass jumping model acts more accurately for the robot. Moreover, three-point supporting composed of two-wheel driving assembly and the supporting leg balances the robot in quiescent condition, and the front rake can be adjusted by the three-point supporting to get enough horizontal distance. Considering all the factors above, a nonlinear spring-single mass intermittent jumping model (see Fig 4) is established for the robot.

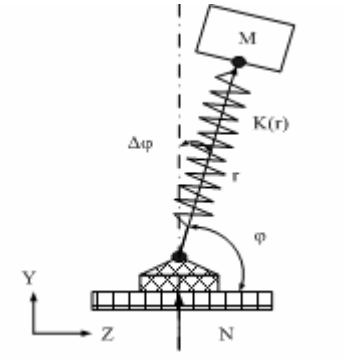

Fig. 4. Jumping model of the robot

r is the original length of non-linear spring, and φ is the front rake of robot. Then the five-shank mechanism is equivalent to the non-linear spring whose elastic coefficient is $K(r)$, just as expression (3). Some processes and transients which are important to jumping performance will be analyzed.

4.1 Process on the Ground

Assume that the point in which the potential energy is zero lies on the ground, then the kinetic energy and potential energy of the robot in the process on the ground are:

$$\begin{cases} K = \dfrac{1}{2} M\left(\dot{r}^2 + (r\dot{\varphi})^2\right), \\ V_1 = Mgr\sin\varphi, \\ V_2 = \dfrac{1}{2} K(r)(r_0 - r)^2. \end{cases} \tag{4}$$

So the Lagrange's equation is:

$$L = \frac{1}{2} M\left(\dot{r}^2 + (r\dot{\varphi})^2\right) - Mgr\sin\varphi - \frac{1}{2} K(r)(r_0 - r)^2.$$

Substitute it into the second Lagrange's equation:

$$\frac{d}{dt}\left(\frac{\partial L}{\partial \dot{x}_i}\right) - \frac{\partial L}{\partial x_i} = 0.$$

After simplification, differential motion equations of the robot are:

$$\begin{cases} M\cdot\ddot{r}-M\cdot r\dot{\varphi}^2+Mg\sin\varphi-K(r)(r_0-r)=0, \\ \dfrac{d\left(Mr^2\dot{\varphi}\right)}{dt}+Mgr\cos\varphi=0. \end{cases} \tag{5}$$

With the consideration of the fact that the inertial rotation hardly functions on the movement because of the attitude adjusting, it is supposed that the robot neglects its inertial rotation and the φ is a constant. So the equation (5) can be simplified into:

$$M\cdot\ddot{r}+Mg\sin\varphi+K(r)(r-r_0)=0.$$

If $\omega^2=K(r)/M$, the initial condition is $r(0)=r_0$ (r_0 is the original length of non-linear spring), $\dot{r}(0)=0$. After the differential equation is solved, expression of the robot's motion during the process on the ground is:

$$r(t)=\left(\frac{K(r)L_0}{\omega M}-\frac{g\sin\varphi}{\omega}\right)\sin(\omega t)+r_0\cos(\omega t). \tag{6}$$

4.2 Jumping Transient

Assume that the robot doesn't jump beforehand, the robot in jumping transient satisfies the criteria:

$$r(t')=r_0,\ \dot{r}(t')>0.$$

A function is introduced:

$$\Theta(r^*,r_0,\varphi,M,K)=\int_{r_0}^{r^*}K(r)(r_0-r)dr-Mg(r^*-r_0)\sin\varphi.$$

In it r^*-r_0 is the deformation of non-linear spring, and φ is the front rake of the robot.

When $F_y=Mg\sin\varphi$, in Fig 3 there are two corresponding points (F_y,r_1) and (F_y,r_2), and $r_1<r_2$. When $r^*\in(r_1,r_2)$, the five-shank mechanism can offer larger force than the weight of the robot, so the jumping criteria is:

$$\begin{cases} \Theta(r^*,r_0,\varphi,M,K)>0, \\ r_1<r^*<r_2. \end{cases} \tag{7}$$

If viscous damper and friction are ignored, the energy conservation equation is:

$$\int_{r_0}^{r^*}K(r)(r_0-r)dr=\frac{1}{2}M(v^*)^2+Mg(r^*-r_0)\sin\varphi.$$

In it, v^* is the initial off-ground velocity, and r^* is the length of the five-shank mechanism in Y direction when off-ground.

4.3 Aerial Process

After jumping over, the robot is in parabolic motion under the effect of its own weight, so the equation of motion for the robot is:

$$\begin{cases} Y(t) = v^* t \sin\varphi - \dfrac{1}{2} g t^2 + r_0 \sin\varphi, \\ Z(t) = v^* t \cos\varphi. \end{cases} \tag{8}$$

4.4 Jumping Height

Under the condition that the efficiency is ignored, the robot can move to the highest point when all its elastic potential energy turns into gravitational potential energy. It satisfies:

$$Mg\,(H_{\max} - r^*) = \int_{r_0}^{r^*} K(r)(r_0 - r)\,dr - \frac{1}{2} M\,(v^* \cos\varphi)^2. \tag{9}$$

So the maximum jumping height of the robot is:

$$H_{\max} = \frac{1}{Mg} \int_{r_0}^{r^*} K(r)(r_0 - r)\,dr - \frac{1}{2g}(v^* \cos\varphi)^2 + r^*. \tag{10}$$

The maximum jumping height $H_{\max}$ is the most important parameter of the wheeling-hopping combination scout robot. According to expression (10), it closely relates to the initial off-ground velocity v^*, the length of the five-shank mechanism in Y direction r^*, and the front rake of robot φ.

The front rake φ is determined by the comprehensive requirements for both jumping height and horizontal distance. According to jumping criteria of expression (7), it is necessary to make r^* be close to r_2 in order to get a higher jumping height. At the same time, an initial velocity is needed to avoid the robot jumping beforehand. So an elastic buffer set in the five-shank mechanism with the thickness of $r_2 - r_3$ is designed to absorb the deformation from r_2 to r_3 in direction Y. And then, just as the five-shank mechanism gets r_3, the robot gains the largest $F_{\max}$ to jump over. Thus there are larger impact force and jumping velocity for the robot to get an ideal height.

5 Simulation Analysis and Jumping Experiment of the Robot

A simulation analysis is carried out with the software ADAMS to validate the jumping performance of the robot. The parameters of the spring are as follows: the elastic coefficient of spring $k = 5\text{N/mm}$, the damping of the spring $C = 0.05\text{Ns/mm}$, the original length of the spring $L_0 = 30\text{mm}$, and the front rake of robot $\varphi = 60^0$. Then the height-time curve of robot's barycenter is shown in Fig 5.

From Fig 5 we can see that the maximum jumping height of the robot is about 150mm. From equation (10) we got theoretical maximum jumping height, 180mm, which is close to the simulation value.

In the jumping experiment, when four springs with elastic coefficient $k = 1.2\text{N/mm}$ are used for the five-shank mechanism, the maximum jumping height of

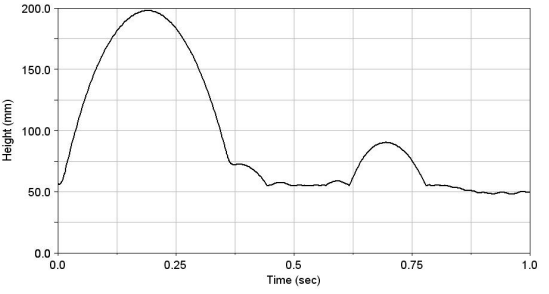

Fig. 5. The height-time curve of robot's barycenter

the robot is 75mm . Contrasted with simulation and theoretical value, the utilization ratio of the energy is only 41%. It is believed that the reason lies in energy loss caused by non-rigid impacting between jumping leg and ground, friction of driving assembly, and damping.

6 Conclusion

A wheeling-hopping combination scout robot was developed in this paper. The robot was equipped with a novel five-shank hopping mechanism, and the nonlinear characteristics of the mechanism were analyzed. Then the nonlinear character was used in the proposed nonlinear spring-mass model for the robot to deduce the rules of robot's movement and to optimize the jumping performance. Finally, a simulation analysis and experiments of the robot's movement were carried out. The results show that the robot has locomotivity and survival ability as strong as a scout robot. After further weight losing and structure optimizing, a more smart and low cost scout robot can be got and used as wireless sensor network node, which plays an important part in military reconnaissance, urban search and rescue, among other things.

Acknowledgements

This work was supported by the National High Technology Research and Development Program of China under grant No. 2007AA041501 and Program for Changjiang Scholars and Innovative Research Team in University under grant No. IRT0423.

References

1. Stoeter, S.A.: Nikolaos Papanikolopoulos. Autonomous Stair-Climbing With Miniature Jumping Robots. IEEE Transactions on systems, man and cybernetics 35, 313–324 (2005)
2. Pearce, J.L., Rybski, P.E., Stoeter, S.A., Papanikolopoulos, N.: Dispersion Behaviors for a Team of Multiple Miniature Robots. In: Proceedings of the 2003 IEEE International Conference on Robotics & Automation Taipei, pp. 1158–1163 (2003)

3. Zhuangzhi, L., Wenming, X., Jianying, Z., Hongtao, W.: Research On Jumping Robots. Robot 25, 568–569 (2003)
4. Xu-feng, X., Wen-jie, G., Yong-hong, Z.: Gait Stability of Jumping Kangaroo Robot Based on Spring-mass Model. Robot 28, 489–493 (2006)
5. Xiao-chuan, Y., Hai-la, H., Pei-cong, W., Ke-qiang, Z.: Jumping Machine Design and Dynamics Analysis of Hopping Robots. Journal of Xiamen University (Natural Science) 45, 505–507 (2006)
6. Hai-la, H., Pei-cong, W., Ke-qiang, Z.: Jumping Machine Design and Dynamics Analysis of Hopping Robots. Journal of Xiamen University (Natural Science) 45, 505–507 (2006)
7. Yan-Zhu, L.: Qualitative Analysis for a One-legged Hopping Robot. Mechanics And Practice 17, 19–20 (1995)